



# NATIONAL INSTITUTE FOR FUSION SCIENCE

## Power Deposition by Neutral Beam Injected Fast Ions in Field-Reversed Configurations

T. Takahashi, T. Kato, N. Iwasawa and Y. Kondoh

(Received - Mar. 19, 2004 )

NIFS-798

Apr. 2004

**RESEARCH REPORT**  
NIFS Series

This report was prepared as a preprint of work performed as a collaboration research of the National Institute for Fusion Science (NIFS) of Japan. The views presented here are solely those of the authors. This document is intended for information only and may be published in a journal after some rearrangement of its contents in the future.

Inquiries about copyright should be addressed to the Research Information Center, National Institute for Fusion Science, Oroshi-cho, Toki-shi, Gifu-ken 509-5292 Japan.

E-mail: [bunken@nifs.ac.jp](mailto:bunken@nifs.ac.jp)

**<Notice about photocopying>**

In order to photocopy any work from this publication, you or your organization must obtain permission from the following organization which has been delegated for copyright for clearance by the copyright owner of this publication.

Except in the USA

Japan Academic Association for Copyright Clearance (JAACC)  
41-6 Akasaka 9-chome, Minato-ku, Tokyo 107-0052 Japan  
TEL:81-3-3475-5618 FAX:81-3-3475-5619 E-mail:[naka-atsu@muj.biglobe.ne.jp](mailto:naka-atsu@muj.biglobe.ne.jp)

In the USA

Copyright Clearance Center, Inc.  
222 Rosewood Drive, Danvers, MA 01923 USA  
Phone: (978) 750-8400 FAX: (978) 750-4744

# Power deposition by neutral beam injected fast ions in Field-Reversed Configurations

Toshiki Takahashi, Takayuki Kato, Naotaka Iwasawa\* and Yoshiomi Kondoh

*Department of Electronic Engineering, Gunma University, Kiryu, Gunma 376-8515, Japan*

*\* Satellite Venture Business Laboratory, Gunma University, Kiryu, Gunma 376-8515, Japan*

Effects of Coulomb collisions on neutral beam (NB) injected fast ions into Field-Reversed Configuration (FRC) plasmas are investigated by calculating the single particle orbits, where the ions are subject to the slowing down and pitch angle collisions. The Monte-Carlo method is used for the pitch angle scattering, and the friction term is added to the equation of motion to show effects of slowing down collision such as the deposited power profile. Calculation parameters used are relevant to the NB injection on the FRC Injection Experiment (FIX) device. It is found that the dominant local power deposition occurs in the open field region between the X-point and the mirror point because of a concentration of fast ions and a longer duration travel at the mirror reflection point. In the present calculation, the maximum deposited power to the FRC plasma is about 10 % of the injected power. Although the pitch angle scattering by Coulomb collision destroys the mirror confinement of NB injected fast ions, this effect is found negligible. The loss mechanism due to non-adiabatic fast ion motion, which is intrinsic in non-uniform FRC plasmas, affects much greater than the pitch angle scattering by Coulomb collision.

**Keywords:** Field-Reversed Configuration, neutral beam injection, Monte Carlo method, slowing down collision, power deposition, non-adiabatic motion

## I. INTRODUCTION

The confinement of a Field-Reversed Configuration (FRC) plasma is anomalous<sup>1</sup>; in both the theoretical and experimental investigations, it is a major issue for the FRC plasma as well as the global stability against the tilt mode<sup>2-9</sup>. Besides the anomalous transport coefficients (i.e., the resistivity, diffusivity, and viscosity), the steep density gradient and considerable current density at the separatrix cause a deleterious transverse flow; these are shown in an experimental observation of a rapid decaying FRC's separatrix radius in a few 100  $\mu\text{s}$ .<sup>10</sup> In the case of the resistive plasma, for instance, there exists the perpendicular flow velocity written in the form:  $\mathbf{u}_\perp = -\eta(\mathbf{j} \times \mathbf{B})/B^2$ , where  $\mathbf{u}_\perp$  is the perpendicular flow velocity,  $\eta$  is the resistivity,  $\mathbf{j}$  is the current density, and  $\mathbf{B}$  is the magnetic field. The theoretical study<sup>11</sup> shows that the hollow current profile (i.e., the small  $\mathbf{j}$  at the magnetic axis and the large  $\mathbf{j}$  at the

separatrix) promotes the stability, and recent particle simulation<sup>9</sup> presents that the FRC plasmas are relaxed to have the hollow current profile; this enhances the transverse transport. Since the inhomogeneity is intrinsic in the high- $\beta$  FRC plasmas, for development of an FRC-based fusion reactor a technique to control the profile and to improve the confinement is indispensable to investigate.

The Neutral Beam Injection (NBI) into the FRC plasma has been carried out on the FIX (FRC Injection Experiment) device<sup>12</sup> at Osaka University so as to improve the confinement.<sup>10,13-16</sup> In the FIX device, the FRC plasma is formed in the formation section and translated to the confinement chamber. The Neutral Beam (NB) particles are injected obliquely at an angle of about 19 degree to the geometric axis before and in the translation phase. The experimental results showed that the NBI is effective to prolong the FRC lifetime estimated by the e-folding time

of the separatrix radius. According to Ref. 16, reduction of the level of global wobble motion is found by the experiment, and therefore, the energy and particle losses due to plasma-wall interaction may be suppressed. They proposed that an ion ring current sustained by the NB injected fast ions in the neighborhood of the field-null X-point suppresses the FRC core plasma precession motion around the geometric axis because of the Lorentz attraction force between the ion ring current and the toroidal current. By the NBI, however, the controllability of the current density has never been reported as yet in the FRC experiment.

In Ref. 17, we calculated orbits of NB injected fast ions into the FRC plasma in equilibrium state. It has been shown that the fast ion exhibits a non-adiabatic motion due to non-uniformity of the FRC plasma; the scale length of magnetic field variation is comparable to the Larmor radius of fast ions. Even when a strong mirror field is applied in order to reduce the end loss rate of fast ions, the orbit loss on the wall surface has been found not to be suppressed; this is clarified that the accessibility of fast ion to the wall surface and the non-adiabaticity in its motion. The accessibility to the wall surface in a fixed equilibrium magnetic field is controllable by the injection beam energy. Hence, parametric surveys of the most effective beam energy in terms of the deposition power and driven current by fast ions are important. The collisions between the fast ions and plasma particles, however, are neglected in Ref. 17. Therefore, direct comparison of our results with those from experiments is difficult. In the present paper, the slowing-down collision is considered as a friction term in the equation of motion of fast ions. The fast ion confinement is affected by the pitch-angle scattering, which may cause more rapid orbit loss on the wall. Thus the effects of this scattering should be analyzed by a detailed calculation. A Monte Carlo method is employed in order for the pitch-angle scattering to be taken into account in the fast ion orbit calculation.

The organization of this paper is as follows: In Sec. II, we will describe the calculation of fast ion orbit

considering the Coulomb collisions and explain how to measure local power deposition. Calculated power deposition profile and effects of Coulomb collision, in particular the pitch angle scattering is presented in Sec. III. Section IV is devoted to summarize conclusions.

## II. COMPUTATIONAL MODEL

Computation is carried out mainly for the NB injection experiment in the FIX device. Equilibria of FRC, which are obtained by solving the Grad-Shafranov equation, and NB injection parameters are the same as Ref. 17. In order for the pressure profile in the edge layer to coincide with the experimental results seen in Ref. 18, the separatrix beta value and width of edge layer on the midplane are set to 0.53 and 8 cm respectively. The mirror ratio is controlled by the parameter of boundary condition of the Grad-Shafranov equation  $R_\psi = |\psi(r_w, z_{\text{mir}})/\psi_w|$ , where  $\psi_w$  is the flux function at the wall and midplane. Assuming uniform magnetic field both on the midplane and outside the separatrix  $B_0$  and on the mirror end throat  $B_M$ , the customary mirror ratio  $R_M \equiv B_M/B_0$  is  $R_M = (1 - x_s^2)R_\psi$ , where  $x_s$  is the ratio of the separatrix radius to the wall radius on the midplane. Typical  $x_s$  in our calculation is about 0.58, then  $R_M \approx 0.67R_\psi$ . Contours of calculated pressure are shown in Fig. 1, where values of the normalized pressure  $p/p_0 : p_0 = |\psi_w|^2 / (2\mu_0 r_w^2)$  are indicated. The values of  $R_\psi$  is (a) 2.0 and (b) 10, and the normalized pressure at the separatrix is set to be 5.0 for both cases. The obtained separatrix elongation  $E_s \equiv (\ell_s/2)/r_s$ , where  $\ell_s$  is the separatrix length and  $r_s$  is the separatrix radius, is 5.8 for  $R_\psi = 2$  and 4.6 for  $R_\psi = 10$ , and the racetrack separatrix shape can be clearly seen here. It is shown that a strong mirror field contracts the edge layer near the mirror end.

### A. Beam Ion Orbits with Coulomb Collisions

After the ionization process, the fast ions move in a prescribed equilibrium field without an electric field,

which is calculated from the Grad-Shafranov equation. The equation of motion for fast ions is written in the form:

$$m \frac{d\mathbf{v}}{dt} = q(\mathbf{v} \times \mathbf{B}) - m \nu_{sl} \mathbf{v}, \quad (1)$$

where  $m$  and  $q$  are the mass and charge of the fast ion (i.e., proton), respectively. The friction force due to the slowing down collision is taken into account in Eq (1). The slowing down collision frequency  $\nu_{sl}$  is

$$\nu_{sl} = \sum_{\beta} \frac{n_{\beta} q_{\alpha}^2 q_{\beta}^2 \Lambda}{4\pi \epsilon_0^2 m_{\alpha}^2 v_{\alpha}^3} \left(1 + \frac{m_{\alpha}}{m_{\beta}}\right) \eta(x) \quad (2)$$

$$\eta(x) = \frac{2}{\sqrt{\pi}} \int_0^x e^{-t} \sqrt{t} dt, \quad x \equiv \frac{m_{\beta} v_{\alpha}^2}{2kT_{\beta}}$$

where  $\Lambda$ ,  $v$ ,  $n$  and  $T$  are the Coulomb logarithm, the speed, the number density and the temperature in Kelvin, respectively. The subscript  $\alpha$  means the beam ion and  $\beta$  stands for a species of background particles. The typical value of Coulomb logarithm is about 13 for the NB injection experiment in the FLX device. In the present calculation, the temperature is assumed to be uniform, and here  $T_i = 100$  eV and  $T_e = 50$  eV. Variation of the plasma density is therefore calculated from the equilibrium pressure as  $n(r, z) = p(r, z)/(T_i + T_e)$ .

This slowing down frequency has two useful limits:

$$\nu_{sl} = \begin{cases} \sum_{\beta} \frac{n_{\beta} e_{\alpha}^2 e_{\beta}^2 \Lambda}{8\sqrt{2}\pi \epsilon_0^2 \sqrt{m_{\alpha}}} \left(1 + \frac{m_{\alpha}}{m_{\beta}}\right) E^{-3/2} \\ \quad \text{for } v_{\alpha}^2 \gg \frac{2kT_{\beta}}{m_{\beta}}, E = \frac{1}{2} m_{\alpha} v_{\alpha}^2 \\ \sum_{\beta} \frac{n_{\beta} e_{\alpha}^2 e_{\beta}^2 \Lambda}{3\pi^{3/2} \epsilon_0^2 m_{\alpha}^2} \left(1 + \frac{m_{\alpha}}{m_{\beta}}\right) \left(\frac{m_{\beta}}{2kT_{\beta}}\right)^{3/2} \\ \quad \text{for } v_{\alpha}^2 \ll \frac{2kT_{\beta}}{m_{\beta}}. \end{cases}$$

When the background particles are electrons alone, the slowing down time  $1/\nu_{sl}$  estimated by Eq. (1) is  $370 \mu\text{s}$  for the beam energy of 10 keV. On the other hand  $1/\nu_{sl}$  is 11 ms for the background deuterium ions, which is about 30 times longer than for the electrons case. Therefore, the slowing down due to electrons is found to be dominant. The beam ion orbit is traced by a numerical integration of Eq. (1). In addition to the slowing down collision, the

pitch angle scattering is also taken into account in the present study. According to Ref. 19, the Monte Carlo method is employed for simulating the pitch angle scattering. The pitch angle is changed as follows:

$$\lambda_n = \lambda_0 (1 - \nu_p \tau) \pm \left[ (1 - \lambda_0^2) \nu_p \tau \right]^{1/2} \quad (3)$$

where,  $\lambda \equiv v_{\parallel} / v = \cos \theta_p$  and  $\nu_p$  is the pitch angle collision frequency:

$$\nu_p = \sum_{\beta} \frac{n_{\beta} q_{\alpha}^2 q_{\beta}^2 \Lambda}{8\pi \epsilon_0^2 m_{\alpha}^2 v_{\alpha}^3} \left[ \left(1 - \frac{1}{2x}\right) \eta(x) + \frac{d\eta}{dx} \right] \frac{1}{\pi^2} \quad (4)$$

and  $\tau$  is the time interval for generating the random number to determine which sign in Eq. (3) is applied. In the present study, the characteristic beam ion cyclotron time  $1/\omega_{ci} \equiv m r_w^2 / (q |\psi_w|) = 2m / [q B_0 (1 - x_s^2)]$  is chosen as  $\tau$  in order for the non-dimensional value  $\nu_p \tau$  to be much smaller than unity. The typical collision frequencies of beam protons at a given their energy is shown in Fig. 2, where subscript e and i stand for the background electrons and ions respectively. For the pitch angle scattering,  $\nu_{pi}$  is found about 4 times higher than  $\nu_{pe}$ , and thus the pitch angle scattering between beam protons and background deuterium ions is dominant. When  $B_0 = 0.05$  T, the NB injection energy  $E_b = 10$  keV, and the density  $n = 5.0 \times 10^{19} \text{ m}^{-3}$ , the value of  $\nu_{pi} \tau$  is about  $1.86 \times 10^{-6}$ .

When a generated random number  $R$  is ranging in  $0 < R \leq 0.5$ , the plus sign in Eq. (3) is employed for pitch angle diffusion; the minus sign is used for the else case  $0.5 < R \leq 1$ . As we use the cylindrical coordinates system to describe the equation of motion, the pitch angle should be expressed by  $B_r, B_z$  and  $v_r, v_{\theta}, v_z$ . The relation is defined in the following way:

$$\begin{aligned} \alpha &\equiv \tan^{-1}(B_r / B_z), \quad v \equiv \sqrt{v_r^2 + v_{\theta}^2 + v_z^2} \\ v_{\parallel} &= v \cos \theta_p, \quad v_{\perp} = v \sin \theta_p \\ v_r &= v_{\parallel} \sin \alpha + v_{\perp} \cos \alpha \\ v_z &= v_{\parallel} \cos \alpha - v_{\perp} \sin \alpha \\ v_{\theta} &= v_{\perp} \sin \varphi, \quad v_{\perp} = v_{\perp} \cos \varphi. \end{aligned} \quad (5)$$

The geometry of the velocity and magnetic field in

the  $r-z$  plane is shown in Fig. 3, where  $\alpha$  is the angle between the magnetic field line and the geometric axis (i.e.,  $z$ -axis),  $v_{\perp 1}$  is the perpendicular velocity projected onto the  $r-z$  plane, and  $v_{\parallel}$  is the parallel velocity. The gyro-phase  $\varphi$  that can be described in the perpendicular plane to the magnetic field is shown in Fig. 4. Although the pitch angle  $\theta_p$  is changed due to the collision, the gyro-phase  $\varphi$  however is assumed to remain the same value at the instance of the collision. If we know  $v$ ,  $\theta_p$ ,  $\varphi$ , and  $\alpha$ , the velocity components  $v_r$ ,  $v_\theta$ , and  $v_z$  that are necessary for the calculation of fast ion orbit are all determined.

### B. Power deposition by fast ions

Due to the slowing down collision, fast ions gradually lose their kinetic energy. The lost kinetic energy is deposited to the plasma particles, dominantly to electrons, and FRC plasma is heated through a thermalization process. We will calculate local energy deposition power by fast ions. Equation (3) is equivalent to

$$\frac{dE}{dt} = -2v_{s1}E, \quad E = \frac{1}{2}mv^2$$

Thus the energy loss of a fast ion for  $\Delta t$  is

$$\Delta E = -2v_{s1}E\Delta t$$

The deposition energy to plasma electrons is then  $-\Delta E$  by a test fast ion. In order to compare the deposition power with experimental results of FIX device, the deposition power is estimated by multiplying a weight  $w$ :

$$\Delta P [\text{W}] = \Delta E [\text{J}] \times w [\text{1/sec}]$$

The weight is equal to the particle injection rate  $dN/dt$  divided by the number of test fast ions. A local deposition power is calculated by summing over  $\Delta P$  in each measuring cell, which is shown schematically in Fig. 5. The volume of measuring cell  $\Delta V$  is

$$\Delta V = 2\pi r \Delta r \Delta z$$

A local deposition power per unit volume is therefore  $\Delta P/\Delta V$ . According to this estimation, without an orbit loss on the wall or end loss, total deposition power to FRC plasmas is ideally  $E_b \times dN/dt$ . When the particle injection rate  $dN/dt$  is  $1.5 \times 10^{20}$  [1/sec] ( $\approx 24$  A)

and the beam energy  $E_b$  is 10 keV, then the injection power is 240 kW. However, a fast ion suffers from the orbit loss or end loss, and then the total deposition power decreases.

### III. RESULTS AND DISCUSSION

The injection beam energy and mirror ratio are changed in order to obtain the most effective injection parameter where the NB power deposits to the plasma particles effectively. A test beam ion is traced until it is lost from the end throat or on the wall surface. The mirror ratio is controlled by the parameter  $R_\psi$ . Figures 6 and 7 show the local deposition power profile in  $r-z$  plane (i.e., quarter cross section of FRC confinement device) for the injection energy  $E_b$  of 8 and 10 keV respectively. The particle injection rate  $dN/dt$  is fixed to be  $1.5 \times 10^{20}$  [1/sec]. In the present calculation, the values of  $R_\psi$  are 2, 4, 6, 8, and 10, and the corresponding results are shown from the top of Figs. 6 and 7. The pitch angle collisions (Eq. (3)) are neglected here. The region where is painted by white color shows that the energy of fast ions is highly deposited in the region. The white dashed lines in Figs. 5 and 6 indicate the separatrix. In a case of  $R_\psi = 2$  and of both 8 and 10 keV, almost all of the fast ions are lost directly and the energy of fast ions is deposited only on their single path from the ionization point to the mirror end. Fast ions can excuse deeply in the mirror field region in the case that  $R_\psi = 2$  and 4. Therefore, a stronger magnetic mirror than  $R_\psi$  of 4 is effective to reduce the end loss ions. Dominant power deposition is found to take place outside the separatrix and in the region where fast ions bounce by the magnetic mirror. The axial velocity of ions decrease near the mirror reflection point, and thus the ion reside here for a long duration. Moreover, since fast ion orbits are focused around the mirror region, the fast ion population is larger here than the midplane. Further, the plasma density in the edge region is considerably high in the present equilibrium model. The separatrix beta value  $\beta_s \equiv p_s / p_{ax}$  where  $p_s$  and  $p_{ax}$  are the plasma pressure at the separatrix and at the magnetic axis (i.e., the field-null

O-point) is set to be about 0.53 in the current calculation, which is the identical condition with the experiment carried out on the FIX device.<sup>18</sup> Hence, when the uniform temperature is assumed, the density in the edge layer is high enough to slow down the fast ions. Because of the reasons mentioned above, it appears consequently that the fast ions deposit their energy to the plasma particles in the edge and mirror region of FRC plasma. It is noted that for 8-keV beam ions the highest deposition to plasma particles is occurred in the case of not  $R_\psi = 8$  and 10 but  $R_\psi = 6$ . This is surprising because we believe a higher magnetic mirror confines beam ions better and suppress the end loss rate. The orbit losses on the wall, however, still happen even in the case of higher mirror field. A statistical property of the mirror reflection and sudden change of the pitch angle is important to know how frequent the orbit loss takes place. For  $R_\psi = 10$ , fast ions go frequently toward the wall around the midplane and often suffer from the orbit losses. Resultantly, the deposition power to the plasma is not high.

To see this clearly, we present the total deposition power by fast ions into FRC plasma in Fig. 8(a); it depends on the mirror ratio and injection beam energy. The percentages of deposition power  $P$  against the injection power  $P_{in}$  are presented in Fig. 8(b). Figure 8(c) shows the ratio of the deposited power into electrons  $P_e$  to the total deposited power  $P$ . In Fig. 8, the solid circle, square, diamond, and triangle represent the injection energy  $E_b$  of 8, 10, 12, and 14 keV, respectively. The highest deposition power of about 18.8 kW is achieved at  $R_\psi = 6$  and  $E_b$  of 8 keV; it is about 10 % of the injection power ( $\approx 190$  kW). The peak of deposition power for  $E_b$  of 8 keV is at  $R_\psi = 6$ , for  $E_b$  of 10 keV is at  $R_\psi = 7$ , and for  $E_b$  of 12 keV is at  $R_\psi = 9$ . On the other hand, as the mirror field becomes higher, the deposition power is found to increase gradually for the 14-keV ions. Judging from the accessibility of fast ions to the mirror end, the 8-keV ions can never travel to the end in the case that  $R_\psi \geq 6$ . The 14-keV ions, however, is accessible to the mirror end and is lost until  $R_\psi \approx 10$ . Therefore, as the mirror ratio

increases, the deposition power by the 14-keV ions is increased gradually because of their longer mirror trap. As we mentioned in Sec. II A, the slowing down frequency by electrons is 30 times higher than the one by ions, when the beam energy is 10 keV. Therefore, the energy transferred to the electrons is about 97 % of the total deposited energy. This seems consistent with the result seen in Fig. 8(c). If the beam energy is decreased, the slowing down collision frequency by ions is increased as shown in Fig. 2. This appears slightly for the injection energy of 8 keV and  $R_\psi \geq 4$  because the ratio  $P_e/P$  is decreased. The beam is confined well enough to be slowed down, and then the slowing down by ions becomes remarkable.

We find the highest efficiency is obtained when the beam energy is 8 keV. In Fig. 9, the dependence of trapped fraction of fast ions in percentage  $\alpha$  on the number of mirror reflection  $N_M$  is shown for the highest efficient 8 keV injection. It is found that  $\alpha$  is decreased as the ions experience the mirror reflection. The largest  $\alpha$  is obtained for  $R_\psi = 6$ ; it is consistent with the result seen in Fig. 8. From our previous work<sup>17</sup>, the fast ions are found to be lost on the wall surface due to their non-adiabatic motion, even when a strong mirror field is applied. A non-uniform FRC plasma is the origin of the collisionless pitch angle scattering of NB injected fast ions.

As is shown in Figs. 6 and 7, the beam energy is deposited mainly in the peripheral region; it is not favorable to heat effectively the core plasma. In Fig. 10, the percentage of deposited power inside and outside the separatrix is shown. When  $R_\psi = 2$ , the deposited power is transferred into the interior of the separatrix. At  $R_\psi = 3$ , NB power for  $E_b$  of both 8 keV and 14 keV is distributed equally inside and outside the separatrix, and the power deposited outside the separatrix excesses for  $R_\psi \geq 4$ . As the beam energy is increased, the total deposition power and the internal deposited power are decreased; it is ineffective to heat the core plasma.

To examine the effects of pitch angle scattering by Coulomb collision, we define the parameter of increment (or decrement) of total deposition power  $\xi$  as

$$\xi \equiv \frac{P_p - P}{P} \times 100 \quad [\%].$$

where  $P_p$  is the total deposition power to the plasmas in the case that both the slowing down collision and pitch angle collision are taken into account, and  $P$  is the same as is shown in Fig. 8(a) (i.e., the case that the slowing down collision alone is considered). Dependence of the parameter  $\xi$  on the mirror ratio  $R_\psi$  for various injection energies is shown in Fig. 11. The plots of  $\xi$  are found to be scattered, and then no significant tendency is observed from this figure. Generally, Coulomb collisions enhance a loss rate of fast ions, because they break the fast ions' adiabatic ion motion; this is important for the mirror confinement. However, the fast ions exhibit intrinsically a non-adiabatic motion in non-uniform high-beta FRC plasmas. Resultantly, the beam ion orbit is ergodic, and a change of trajectory by pitch angle collisions is not so important. The present result shows that the effect of Coulomb collision on the power deposition is settled in at most  $-15\% \leq \xi \leq +5\%$ . For  $R_\psi \leq 4$ , the pitch angle collisions increases slightly the deposition power, because they suppress a little beam ion's direct end loss. On the other hand, in the case that  $R_\psi \geq 6$ , pitch angle collisions rather worsen the efficiency of NB injection. Further, fraction of confined fast ions at the number of their mirror reflection is presented in Fig. 12 to find how the Coulomb collisions affect the duration of mirror trap. The calculation is done for (a) the highest efficient case (i.e., 8 keV and  $R_\psi = 6$ ) and for (b) 10 keV and  $R_\psi = 6$ . In Fig. 12, comparison with the collisionless case is made, where the slowing down collisions are also neglected. Although a slight difference between the collisional and collisionless case can be seen, almost the same gradual decrease is found for both 8 and 10 keV.

#### IV. SUMMARY

Effects of Coulomb collisions on neutral beam (NB) injected fast ions into Field-Reversed Configuration (FRC) plasmas have been investigated with the aid of the calculation of single particle orbits. The slowing down and

pitch angle collisions have been taken into account. Injection geometry in the present calculation is similarly arranged to the FIX (FRC Injection Experiment) device. This calculation is done for the beam energy of 8, 10, 12, and 14 keV. It is found that the power of fast ions is deposited dominantly in the open field region between the X-point and the mirror point because of a concentration of fast ions and a longer duration travel at the mirror reflection point. About 40 % of the deposited power into the FRC plasma is found to be delivered inside the separatrix. The highest efficient case is the injection energy of 8 keV and the mirror ratio  $R_\psi = 6$ ; the obtained deposited power to the FRC plasma in this case is 10 % of the injected power (see Fig. 8). Although the pitch angle scatterings destroy the mirror confinement of NB injected fast ions, this effect is found insignificant; it has been shown from a comparison of the trapped fraction of fast ions with and without collisions (cf. Fig. 12). According to our previous work<sup>17</sup>, the non-adiabatic fast ion motion influences much greater than the pitch angle Coulomb collisions.

Recent experiment shows that a global motion of FRC is suppressed by an NB injection, which may improve the confinement of FRC plasmas.<sup>16</sup> In order to clarify the mechanism of the suppression, computational study is needed. A Self-consistent hybrid or particle simulation remains for a future study to reproduce 3 dimensional FRC global motions and its stabilization by NB injected fast ions.

#### ACKNOWLEDGEMENTS

One of the authors (T. T) wishes to acknowledge valuable discussions with Dr. Michiaki Inomoto, Dr. Tomohiko Asai, Dr. Youichi Hirano, Prof. Tsutomu Takahashi, Dr. Naoki Mizuguchi, Prof. Shoichi Ohi, and Prof. Yukihiro Tomita. This work is performed with the support and under the auspices of the NIFS Collaborative Research Program.

<sup>1</sup> M. Tuszewski, Nucl. Fusion **28**, 2033 (1988).

- <sup>2</sup> R. D. Milroy, D. C. Barnes, R. C. Bishop, and R. B. Webster, *Phys. Fluids B* **1**, 1225 (1989).
- <sup>3</sup> R. Horiuchi and T. Sato, *Phys. Fluids B* **1**, 581 (1989).
- <sup>4</sup> N. Iwasawa, A. Ishida, and L. C. Steinhauer, *Phys. Plasmas* **7** 931 (2000).
- <sup>5</sup> E. V. Belova, S. C. Jardin, H. Ji, M. Yamada, and R. Kulsrud, *Phys. Plasmas* **7**, 4996 (2000).
- <sup>6</sup> E. V. Belova, S. C. Jardin, H. Ji, M. Yamada, and R. Kulsrud, *Phys. Plasmas* **8**, 1267 (2001).
- <sup>7</sup> Y. A. Omelchenko, M. J. Schaffer, and P. B. Parks, *Phys. Plasmas* **8**, 4463 (2001).
- <sup>8</sup> D. C. Barnes, *Phys. Plasmas* **9**, 560 (2002).
- <sup>9</sup> H. Ohtani, R. Horiuchi, and T. Sato, *Phys. Plasmas* **10**, 145 (2003).
- <sup>10</sup> T. Asai, Y. Suzuki, T. Yoneda, F. Kodera, M. Okubo, S. Okada, and S. Goto, *Phys. Plasmas* **7**, 2294 (2000).
- <sup>11</sup> L. C. Steinhauer, A. Ishida, and R. Kanno, *Phys. Plasmas* **1**, 1523 (1994).
- <sup>12</sup> A. Shiokawa and S. Goto, *Phys. Fluids B* **5**, 534 (1993).
- <sup>13</sup> T. Asai, Ph.D. thesis, Graduate School of Engineering, Osaka University, Japan, 2001.
- <sup>14</sup> T. Asai, F. Kodera, M. Okubo, S. Okada, and S. Goto, *J. Plasma Fusion Res.* **77**, 1230 (2001).
- <sup>15</sup> S. Okada, T. Asai, F. Kodera, K. Kitano, Y. Suzuki, K. Yamanaka, T. Kanki, M. Inomoto, S. Yoshimura, M. Okubo, S. Sugimoto, S. Ohi, and S. Goto, *Nucl. Fusion* **41**, 625 (2001).
- <sup>16</sup> T. Asai, M. Inomoto, N. Iwasawa, S. Okada, and S. Goto, *Phys. Plasmas* **10**, 3608 (2003).
- <sup>17</sup> T. Takahashi, K. Inoue, N. Iwasawa, T. Ishizuka, and Y. Kondoh, *Losses of neutral beam injected fast ions due to adiabaticity breaking processes in a Field-Reversed Configuration*, to be published in *Phys. Plasmas*.
- <sup>18</sup> T. Ohtsuka, M. Okubo, S. Okada, and S. Goto, *Phys. Plasmas* **5**, 3649 (1998).
- <sup>19</sup> A. H. Boozer and G. K. Petravich, *Phys. Fluids* **24**, 851 (1981).

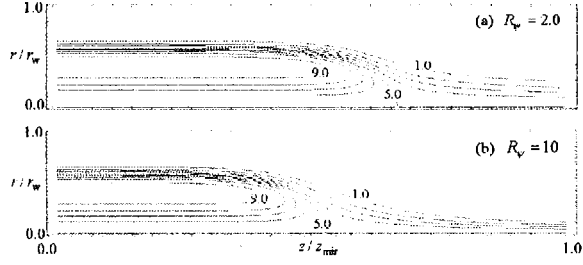


FIG. 1. The contour lines of the plasma pressure  $p$  normalized by  $|\psi_w|^2 / (2\mu_0 r_w^4)$  in the quarter cross section of the confinement region in  $r$ - $z$  plane for the case of (a)  $R_\psi = 2$  and (b)  $R_\psi = 10$ . The contour intervals are 1.0.

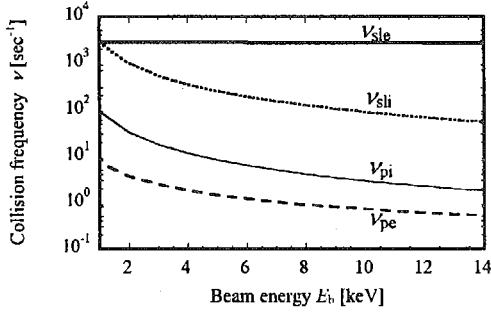


FIG. 2. The slowing down collision frequency  $\nu_{sl}$  and the pitch angle scattering frequency  $\nu_p$  of beam protons vs. the beam energy  $E_b$ . Here  $T_i = 100$  eV,  $T_e = 50$  eV, and  $n = 5 \times 10^{19} \text{ m}^{-3}$ . Thick solid line  $\nu_{sle}$  is for slowing down by electrons, dotted line  $\nu_{sli}$  is for by slowing down by ions, thin solid line  $\nu_{pi}$  is for pitch angle scattering by ions, and dashed line  $\nu_{pe}$  is for pitch angle scattering by electrons.

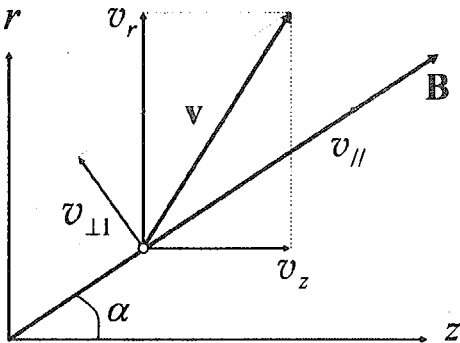


FIG. 3. Magnetic field and beam ion velocity projected onto  $r$ - $z$  plane.

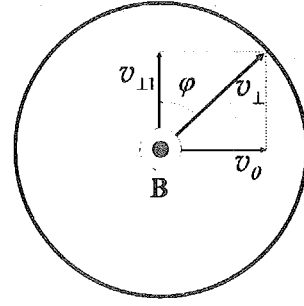


FIG. 4. Gyro-phase and geometry of perpendicular velocity projected onto the perpendicular plane to magnetic field.

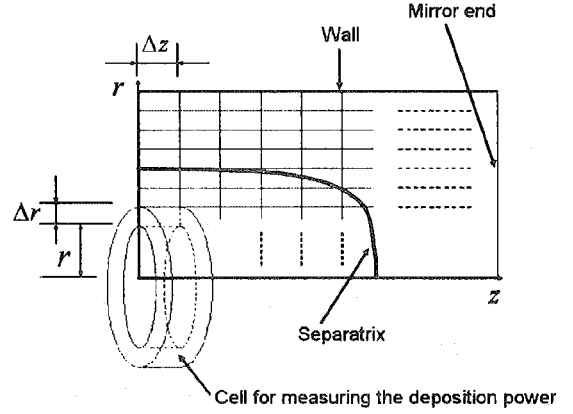


FIG. 5. Schematic drawing of simulation space

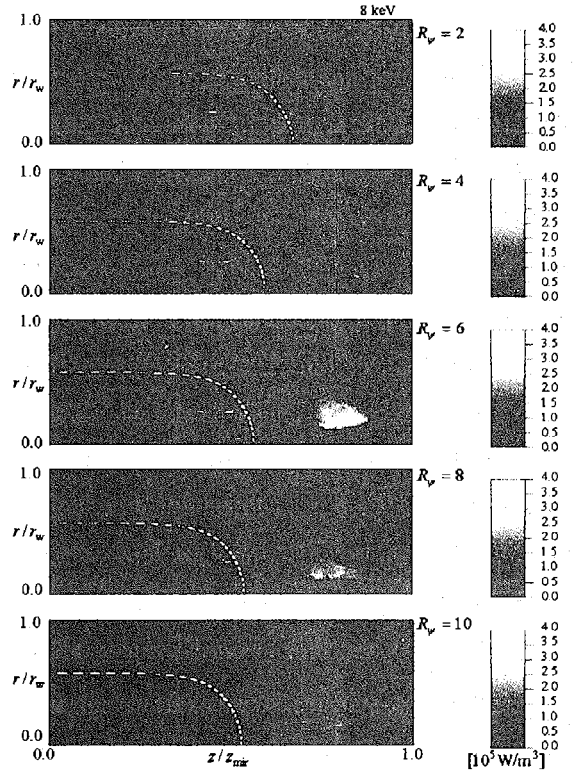


FIG. 6. Local power deposition profile in  $r$ - $z$  plane (i.e., quarter cross section of confinement region). NB injection energy is 8 keV. White dashed line indicates the separatrix.

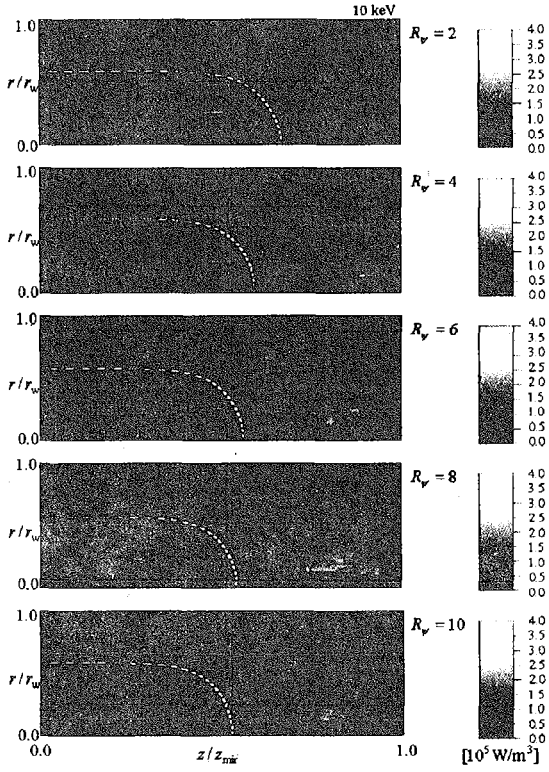


FIG 7. Local power deposition profile in  $r$ - $z$  plane (i.e., quarter cross section of confinement region). NB injection energy is 10 keV. White dashed line indicates the separatrix.

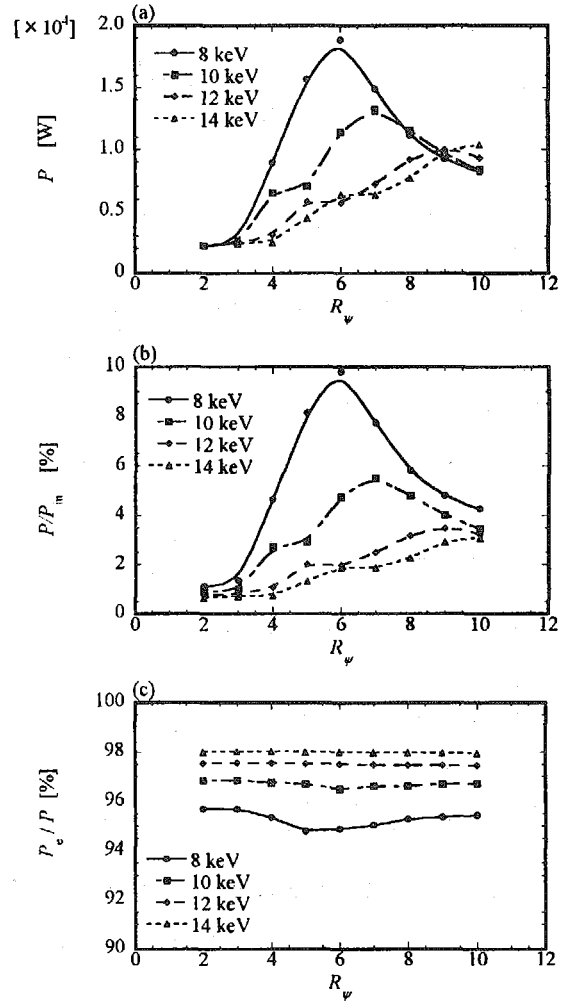


FIG 8. The deposition power by NB injected protons vs. the mirror ratio. (a) Total deposition power into the FRC plasma, (b) the ratio of deposited power to the injected power, and (c) the ratio of the deposited power into electrons. The lines are drawn smoothly by the least square method.

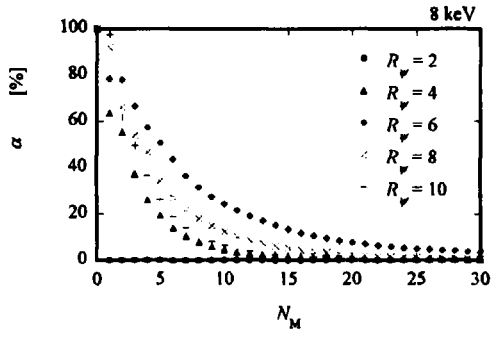


FIG. 9. Relation between confined fast ion fraction in percentage and the number of mirror reflection. Injection beam energy is 8 keV here. The values of mirror ratio control parameter  $R_p$  are 2 (solid circle), 4 (solid triangle), 6 (solid diamond), 8 (cross), and 10 (plus).

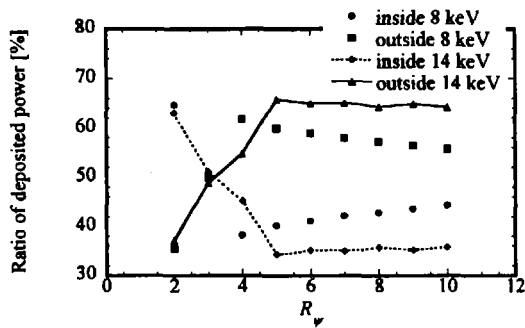


FIG. 10. The ratio of the deposited power inside and outside the separatrix. The lines are drawn to guide the reader's eye.

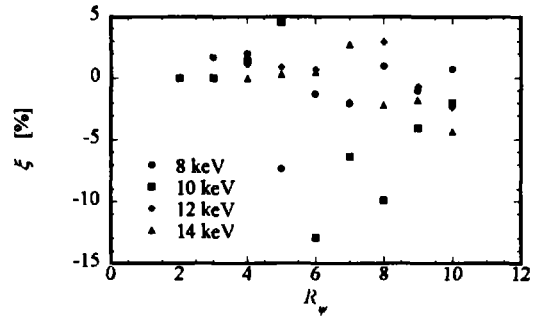


FIG. 11. The mirror ratio dependence of total deposition power increment (decrement)  $\xi$  due to pitch angle collisions for the injected beam energy of 8 keV (solid circle), 10 keV (solid square), 12 keV (solid diamond), and 14 keV (solid triangle).

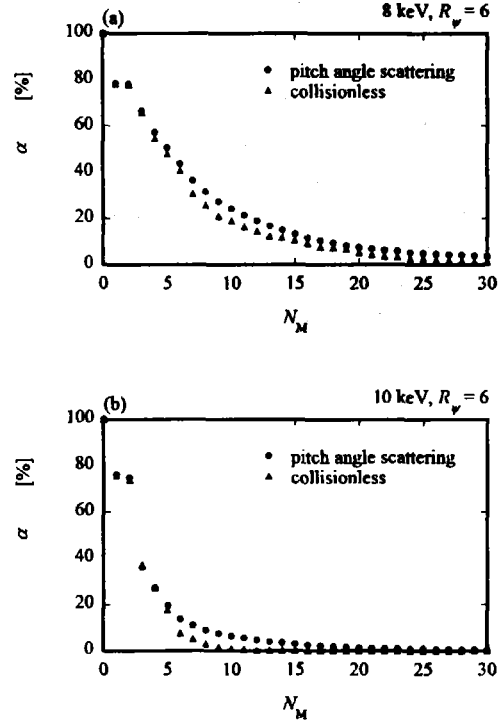


FIG. 12. Relation between confined fast ion fraction in percentage and the number of mirror reflection. Injection beam energies are (a) 8 keV and (b) 10 keV, and the mirror ratio is  $R_p = 6$  for both (a) and (b).

## Recent Issues of NIFS Series

- NIFS-774 K. Itoh, S.-I. Itoh, F. Spineanu, M.O. Vlad and M. Kawasaki  
On Transition in Plasma Turbulence with Multiple Scale Lengths  
May 2003
- NIFS-775 M. Vlad, F. Spineanu, K. Itoh, S.-I. Itoh  
Intermittent and Global Transitions in Plasma Turbulence  
July 2003
- NIFS-776 Y. Kondoh, M. Kondo, K. Shimoda, T. Takahashi and K. Osuga  
Innovative Direct Energy Conversion Systems from Fusion Output Thermal Power to the Electrical One with the Use of Electronic Adiabatic Processes of Electron Fluid in Solid Conductors.  
July 2003
- NIFS-777 S.-I. Itoh, K. Itoh and M. Yagi  
A Novel Turbulence Trigger for Neoclassical Tearing Modes in Tokamaks  
July 2003
- NIFS-778 T. Utsumi, J. Koga, T. Yabe, Y. Ogata, E. Matsunaga, T. Aoki and M. Sekine  
Basis Set Approach in the Constrained Interpolation Profile Method  
July 2003
- NIFS-779 Oleg I. Tolstikhin and C. Namba  
CTBC A Program to Solve the Collinear Three-Body Coulomb Problem: Bound States and Scattering Below the Three-Body Disintegration Threshold  
Aug. 2003
- NIFS-780 Contributions to 30th European Physical Society Conference on Controlled Fusion and Plasma Physics  
(St.Petersburg, Russia, 7-11 July 2003) from NIFS  
Aug. 2003
- NIFS-781 Ya. I. Kolesnichenko, K. Yamazaki, S. Yamamoto, V.V. Lutsenko, N. Nakajima, Y. Narushima, K. Toi, Yu. V. Yakovenko  
Interplay of Energetic Ions and Alfvén Modes in Helical Plasmas  
Aug. 2003
- NIFS-782 S.-I. Itoh, K. Itoh and M. Yagi  
Turbulence Trigger for Neoclassical Tearing Modes in Tokamaks  
Sep. 2003
- NIFS-783 F. Spineanu, M. Vlad, K. Itoh, H. Sanuki and S.-I. Itoh  
Pole Dynamics for the Flierl-Petviashvili Equation and Zonal Flow  
Sep. 2003
- NIFS-784 R. Smirnov, Y. Tomita, T. Takizuka, A. Takayama, Yu. Chutov  
Particle Simulation Study of Dust Particle Dynamics in Sheaths  
Oct. 2003
- NIFS-785 T.-H. Watanabe and H. Sugama  
Kinetic Simulation of Steady States of Ion Temperature Gradient Driven Turbulence with Weak Collisionality  
Nov. 2003
- NIFS-786 K. Itoh, K. Hallatschek, S. Toda, H. Sanuki and S.-I. Itoh  
Coherent Structure of Zonal Flow and Nonlinear Saturation  
Dec. 2003
- NIFS-787 S.I. Itoh, K. Itoh, M. Yagi and S. Toda  
Statistical Theory for Transition and Long-time Sustainment of Improved Confinement State  
Dec. 2003
- NIFS-788 A. Yoshizawa, S.-I. Itoh, K. Itoh and N. Yokoi  
Dynamics and MHD Theory of Turbulence Suppression  
Dec. 2003
- NIFS-789 V.D. Pustovitov  
Pressure-induced Shift of the Plasma in a Helical System with Ideally Conducting Wall  
Jan. 2004
- NIFS-790 S. Koikari  
Rooted Tree Analysis of Runge-Kutta Methods with Exact Treatment of Linear Terms  
Jan. 2004
- NIFS-791 T. Takahashi, K. Inoue, N. Iwasawa, T. Ishizuka and Y. Kondoh  
Losses of Neutral Beam Injected Fast Ions Due to Adiabaticity Breaking Processes in a Field-Reversed Configuration  
Feb. 2004
- NIFS-792 T.-H. Watanabe and H. Sugama  
Vlasov and Drift Kinetic Simulation Methods Based on the Symplectic Integrator  
Feb. 2004
- NIFS-793 H. Sugama and T.-H. Watanabe  
Electromagnetic Microinstabilities in Helical Systems  
Feb. 2004
- NIFS-794 S.I. Kononenko, O.V. Kalantaryan, V.I. Muratov and C. Namba  
Spectral and Angular Characteristics of Fast Proton-Induced Luminescence of Quartz  
Mar. 2004
- NIFS-795 K. Itoh, K. Hallatschek and S.-I. Itoh  
Excitation of Geodesic Acoustic Mode in Toroidal Plasmas  
Mar. 2004
- NIFS-796 A. Shimizu, A. Fujisawa, S. Ohshima and H. Nakano  
Consideration of Magnetic Field Fluctuation Measurements in a Torus Plasma with Heavy Ion Beam Probe  
Mar. 2004
- NIFS-797 M.I. Mikhailov, K. Yamazaki  
Fast Particles Confinement in Stellarators with Both Poloidal-Pseudo-Symmetry and Quasi-Isodynamicity  
Apr. 2004
- NIFS-798 T. Takahashi, T. Kato, N. Iwasawa and Y. Kondoh  
Power Deposition by Neutral Beam Injected Fast Ions in Field-Reversed Configurations  
Apr. 2004